



# Evolution of submarine canyon-fan systems in fault-controlled margins: Insights from physical experiments

Steven Y. J. Lai<sup>1</sup>, David Amblas<sup>2</sup>, Aaron Micallef<sup>3</sup>, Thomas P. Gerber<sup>4</sup>, Hérve Capart<sup>5</sup>,

<sup>1</sup>Department of Hydraulic and Ocean Engineering, National Cheng Kung University, Tainan, Taiwan

5 <sup>2</sup>GRC Geociències Marines, Dept. de Dinàmica de la Terra i de l'Oceà, Universitat de Barcelona, Barcelona, Spain

<sup>3</sup>Marine Geology and Seafloor Surveying, Dept. of Geosciences, University of Malta, Msida, Malta

<sup>4</sup>Equinor - Research and Technology, Austin, Texas, USA

<sup>5</sup>Department of Civil Engineering, National Taiwan University, Taipei, Taiwan

*Correspondence to:* Steven Y. J. Lai (stevenyjlai@mail.ncku.edu.tw)

10

**Abstract.** Different fault settings make the morphology of submarine canyon-fan systems on active margins complex and diverse. In this study we explore the continuum of erosion, transport and sedimentation processes taking place in fault-controlled canyon-fan systems by using physical experiments and a morphodynamic model. Based on morphometric analyses we show how Hack's scaling relationships exist in submarine canyons and fans. The DEM of differences (DoDs) demonstrate the growth patterns and allow to establish relevant relationships between volumes of canyons and their corresponding fans. We reveal strong self-similarities on canyon-fan long profiles and, through a new morphodynamic model, we capture their evolution over time, including the trajectory of internal moving boundaries. We observe that fault slip rate controls the merging speed of coalescent submarine canyon-fan systems and, when coupling fault slip rate with inflow discharge, a competitive influence arises. In this study we also uncover scaling relationships spanned from laboratory to field-scale. Overall, our findings are inspiring and valuable for field investigators and modelers to better interpret and predict the morphological evolution and sedimentary processes of submarine canyon-fan systems in active fault settings.

15  
20

## 1 Introduction

Submarine canyons and fans are main physiographic elements in the deeper reaches of the source-to-sink continuum of sedimentary processes. While submarine canyons are drainage features facilitating the transport of sediment from land and shelf to the deep sea, submarine fans represent its final depositional destination in many cases. These sediments are mainly transported by different forms of gravity flows, including turbidity currents, hyperpycnal flows and dense shelf water cascades (Mulder et al., 1995; Dadson et al., 2005; Canals et al., 2006; Milliman and Kao, 2005; Piper and Normark, 2009; Puig et al., 2014; Talling et al., 2015; Amblas and Dowdeswell, 2018 and references therein). Most of our knowledge about the evolution of submarine canyons and fans come from field survey and interpretations on passive margins, but in fact, the number of

25



30 submarine canyons on active margins is higher than that on passive margins (Harris and Whiteway, 2011) and the occurrence of downslope gravity currents is even more frequent (Dadson et al., 2005; Milliman and Kao, 2005).

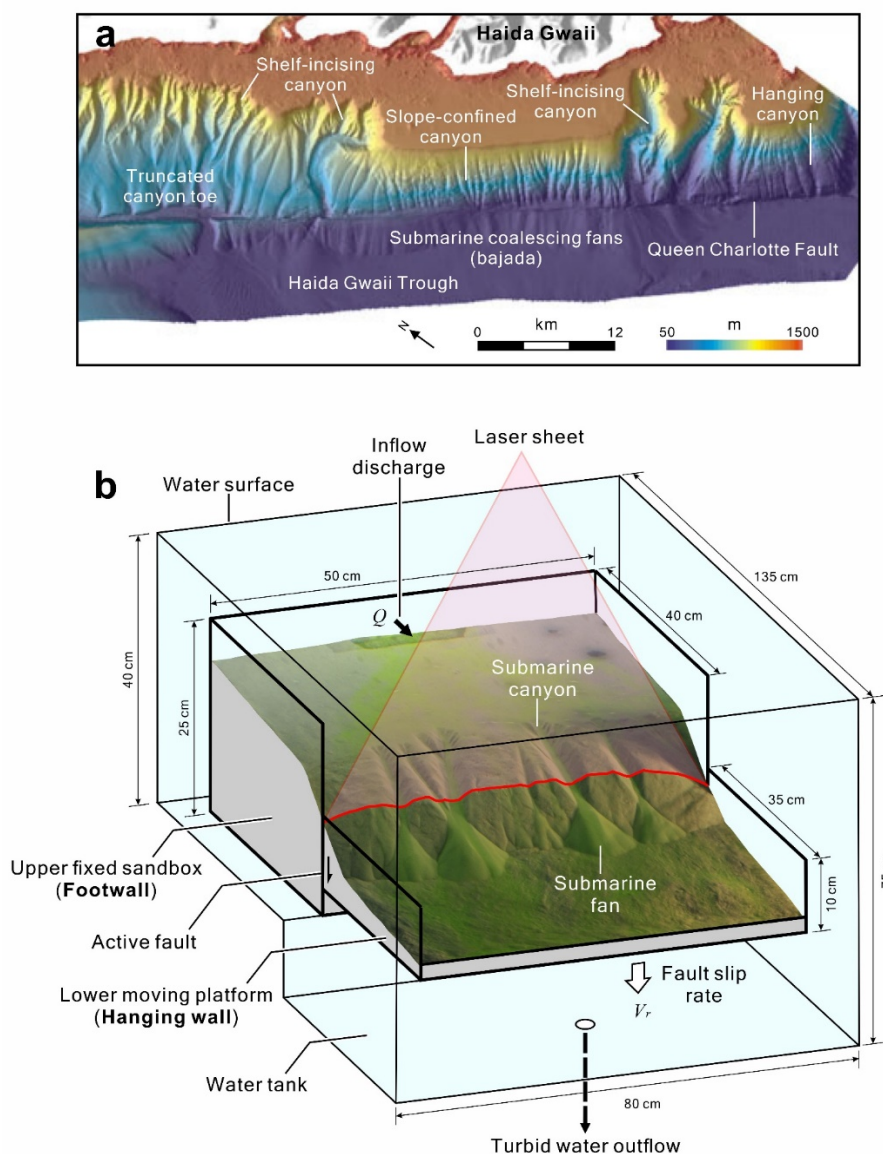
Haida Gwaii, in the northern Pacific coast of Canada, provides good field examples that illustrate the evolution of canyon-fan systems in an active margin (Fig. 1a). Within just 37 km of the Haida Gwaii margin there are 48 submarine canyons showing  
35 different degree of morphological influence by the Queen Charlotte Fault Zone (Harris et al., 2014b). This large strike-slip fault truncates most of the canyon toes and creates numerous slope-confined and hanging canyons, and a series of coalescing fans (bajada)(Harris et al., 2014b). Other similar examples can be found in offshore eastern Taiwan (Hsieh et al., 2020), offshore northern Sicily (Lo Iacono et al., 2014; Gamberi et al., 2015), and along Makran active margin (Bourget et al., 2011).

40 In the past, morphometric analyses for fluvial drainage basins have been used to analyze submarine canyons and fans, and to establish subaqueous scaling relationships and geomorphic process laws. Morphometric analyses can link morphological and sedimentological relationships in the sediment routing system. The classic and widely used river classification (Horton, 1945; Strahler, 1957) and the scaling relationship between river length and catchment area (Hack, 1957) have been widely applied to scale submarine canyon length and its drainage area (Mitchell, 2005; Straub et al., 2007; Tubau et al., 2013; Micallef et al.,  
45 2014). Longitudinal profile analyses were also widely used in submarine canyons to establish general geomorphic process laws (Mitchell, 2005; Gerber et al., 2009; Covault et al., 2011; Amblas et al., 2011, 2012; Brothers et al., 2013). In addition, morphometric analyses were also applied to submarine fan classification to establish scaling relationships between channels and lobes (Pettinga et al., 2018).

50 However, the time scale for forming a submarine canyon-fan system is much longer than a human timescale, making direct measurements of the evolving processes rarely possible. These difficulties have led researchers to turn to experimental studies of submarine canyons and fans. Past physical experiments confirmed that the subaqueous erosional channelized morphology produced by long-lived gravity currents can be reproduced using saline underflow and plastic sediment (Metivier et al., 2005). Subsequent experimental studies also pointed out that slope controls the rate of erosion and the speed of channel incision,  
55 while saline discharge affects the width and depth of submarine canyons (Weill et al., 2014). In different approaches, Lai et al. (2016) demonstrated that laboratory experiments can generate autogenic, deeply incised submarine canyons with well-developed drainage features by using salt water acting on silica paste with submerged stepwise lowering base level. These authors also revealed that the submarine canyon long profile in evolution are time and scale independent. Apart from the canyon experiments, laboratory turbidity currents can generate self-channelized submarine fans with leveed channels that  
60 gradually shift and avulse (Yu et al., 2006). Further experiments showed that repeated turbidity currents can also produce levee-bounded submarine channels and stacked lobes (Cantelli et al., 2011), and that the break in slope controls channel aggradation and lobe architecture (Fernandez et al., 2014).



65 The purpose of this study is to explore the erosion-transport-sedimentation processes involved in the evolution of submarine  
canyon-fan systems in fault-controlled margins. For this we use physical experiments and a morphodynamic model that allow  
to define general geomorphic laws. The aims of this study are: (1) to obtain high-resolution digital elevation models (DEMs)  
for the canyon-fan evolutionary surfaces; (2) to develop laboratory-scale morphometric analyses and to establish scaling  
relationships between parameters; (3) to investigate scale-independent self-similarities in long profiles; (4) to propose a  
morphodynamic model that allow to predict fan volumes based on canyon lengths.



70

Figure 1. (a) Seafloor morphology offshore Haida Gwaii (modified from [Barrie et al., 2013](#) and [Harris et al., 2014b](#)); (b) Experimental setup for studying the evolution of submarine canyon-fan systems in an active fault setting.



## 2 Methods

### 75 2.1 Experimental design

To simulate a basic submarine fault setting that mimics the morphology observed offshore Haida Gwaii, a novel tank (135 cm long, 80 cm wide and 75 cm deep) was designed to recreate the evolution of a submarine fault with 90-degree dip angle (Fig. 1b). This submerged tank consists of an upper fixed sandbox (as a footwall) and a lower moving platform (as a hanging wall). The hanging wall was controlled by a motor with adjustable speed to simulate different fault slip rate ( $V_r$ ). Very fine silica sand ( $d_{50} = 0.1$  mm) and kaolinite (proportion 100:1 by weight, as suggested by Hasbargen and Paola, 2000 and Lai et al., 2016) were well mixed and filled into the submerged sandbox and platform as an erodible substrate. Upstream, different inflows discharge ( $Q$ ) of saturated brine (density  $\rho_{in} = 1200$  kg/m<sup>3</sup>) were used as unconfined downslope gravity currents for modeling long-lived hyperpycnal flows or mud-rich turbidity currents (Métivier et al., 2005; Spinewine et al., 2009; Sequeiros et al., 2010; Weill et al., 2014; Foreman et al., 2015; Lai et al., 2016; 2017).

85

Six experimental runs were performed with different inflow discharges ( $Q = 800$  to 5000 mm<sup>3</sup>/s) and fault slip rates ( $V_r = 0.014$  mm/s to 0.064 mm/s) (Table 1). Each experiment was divided into 7 to 12 successive stages; the stage intervals were 10 min or 5 min, depending on the fault slip rate. Time-lapse photography was used to record the evolution of submarine canyon-fan systems every 5 s for each experiment. Without draining out the ambient water, the inflow was turned off to form a temporarily frozen landscape at each stage end. Then the newly generated submarine landscape was scanned. A topographic imaging system (Lai et al., 2016) was used to construct high-resolution (1 mm x 1 mm) digital elevation models (DEMs), orthorectified images and gradient maps over successive stages.

90

**Table 1. Summary of experimental conditions.**

95

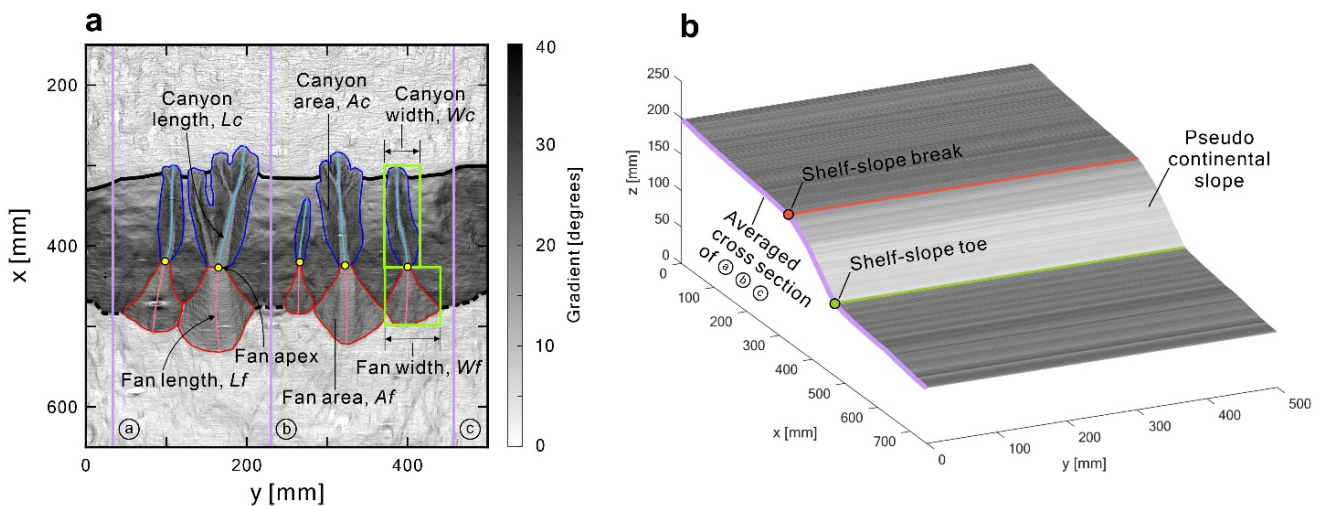
Run	Inflow discharge $Q$ (mm <sup>3</sup> /s)	Fault slip rate $V_r$ (mm/s)	Stage interval (min)	Total stages	Total run time (min)
A1	1600	0.025	10	9	90
A2	1600	0.049	5	9	45
B1	3300	0.026	10	9	90
B2	3500	0.041	5	11	55
C1	5000	0.014	10	12	120
C2	800	0.064	5	7	35



## 2.2 Morphometric definitions

Landscape features of submarine canyon-fan systems were defined prior to morphometric analyses (Fig. 2a). First, the fan apex was defined at the most upstream point of a submarine fan, or the intersection between two fan edge asymptotes. Then, canyon length ( $L_c$ ) was defined as the maximum path from the canyon head to its fan apex; canyon width ( $W_c$ ) was defined as the width of canyon bounding box; canyon area ( $A_c$ ) was the area of canyon drainage. Similarly, fan length ( $L_f$ ) was the maximum path from the fan apex to its fan toe; fan width ( $W_f$ ) was the width of fan bounding box; fan area ( $A_f$ ) was the area fan deposit.

The volumes of submarine canyons and fans can be obtained by subtracting the pseudo continental slope from the DEM of each stage (Fig. 2b). First, three cross sections were extracted from the DEM, which were unaffected by saline underflows (e.g., cross sections a, b and c in Fig. 2a). The averaged cross section was then used to create a pseudo continental slope for that stage (Fig. 2b). Next, the pseudo continental slope was subtracted from the DEM to obtain the DEM of difference (DoD). Negative values represent canyon incision depths; positive values show fan thicknesses. In addition, the ( $x, z$ ) coordinates of the shelf-slope break and shelf-slope toe were recorded from the pseudo continental slope to understand the evolution of these two internal moving boundaries. The moving trajectories will be shown in Section 3.2.



115 **Figure 2. (a) Morphometric definitions of submarine canyon-fan systems. Yellow dots are fan apices. Green rectangles are bounding boxes. Thick black solid line is shelf-slope break; Thick black dash line is shelf-slope toe. (b) Reconstructed pseudo continental slope unaffected by downslope gravity flows.**



## 120 2.3 Morphodynamic model

The formation of a submarine canyon-fan system involves simultaneous erosion and deposition, resembling the knickpoint smoothing process observed in submarine canyons (Mitchell, 2006) and fluvial active faults (Hanks et al., 1984). With this similar concept, a one-dimensional morphodynamic model was developed for describing a fault-controlled submarine canyon-fan evolution, driven by downslope gravity flows (Fig. 3). First, the position of the active fault was set to  $x = 0$ . Then, the submarine canyon-fan evolution was decoupled into two different processes: (1) an evolving continental slope driven by a normal fault (Fig. 3b); (2) a submarine canyon-fan system driven by a downslope gravity flow (Fig. 3c). As the hanging wall continues to fall, the continental slope was mainly formed by avalanching, with its slope kept at the angle of repose ( $S_s = 38^\circ$ ). The retreating shelf-slope break and advancing shelf-slope toe can be described by the following geometric relationships (Eq. (1) and Eq. (2)) (modified from Lai et al., 2016):

$$130 \quad (x, z)_{ssb} = \left( \frac{-H_1}{S_s - S_1}, \frac{S_1 H_1}{S_s - S_1} \right) \quad (1)$$

$$(x, z)_{sst} = \left( \frac{H_2}{S_s - S_2}, \frac{-S_s H_2}{S_s - S_2} \right) \quad (2)$$

where  $H_1$  and  $H_2$  are the upstream and downstream knickpoint heights;  $S_1$  and  $S_2$  are the upstream and downstream far field slopes, respectively.  $S_s$  is the inclination of continental slope.

135 The submarine canyon-fan long profile formed by downslope gravity flows can be described by a diffusion process. Eq. (3) describes the entire submarine canyon-fan long profile  $z(x, t)$ , including both the footwall ( $x_1 = x < 0$ ) and hanging wall ( $x_2 = x > 0$ ):

$$z(x, t) = -H \cdot \operatorname{erf} \left( \frac{x}{2\sqrt{Kt}} \right) - Sx \quad (3)$$

where  $H$  = knickpoint heights (shape factor);  $\operatorname{erf}$  = error function (shape function);  $K$  = diffusivity;  $S$  = far-field slope. The first and second terms on the right-hand side of Eq. (3) account for the variations in bed profile caused by the geomorphic diffusion and initial bed slope, respectively. Diffusion processes on footwall and hanging wall may be different, suggesting that different parameters ( $H_1, K_1, S_1$ ) and ( $H_2, K_2, S_2$ ) can be used for the upstream and downstream canyon-fan long profiles.

To investigate the self-similarity of the evolving canyon-fan long profiles in various settings, the first and second terms on the right-hand side of Eq. (3) were normalized, respectively, by the shape factor  $H$  and the time-varying length scale  $\sqrt{Kt}$ . Then the normalized profiles  $\bar{z}$  is time-varying only as a function of the dimensionless horizontal coordinate  $\sigma (= x/\sqrt{Kt})$  (Capart et al., 2007; Lai and Wu, 2021):

$$\bar{z}(\sigma) = -\operatorname{erf} \left( \frac{\sigma}{2} \right) - S\sigma \quad (4)$$

The comparison between diffusion model and experiments will be presented in Section 3.2.



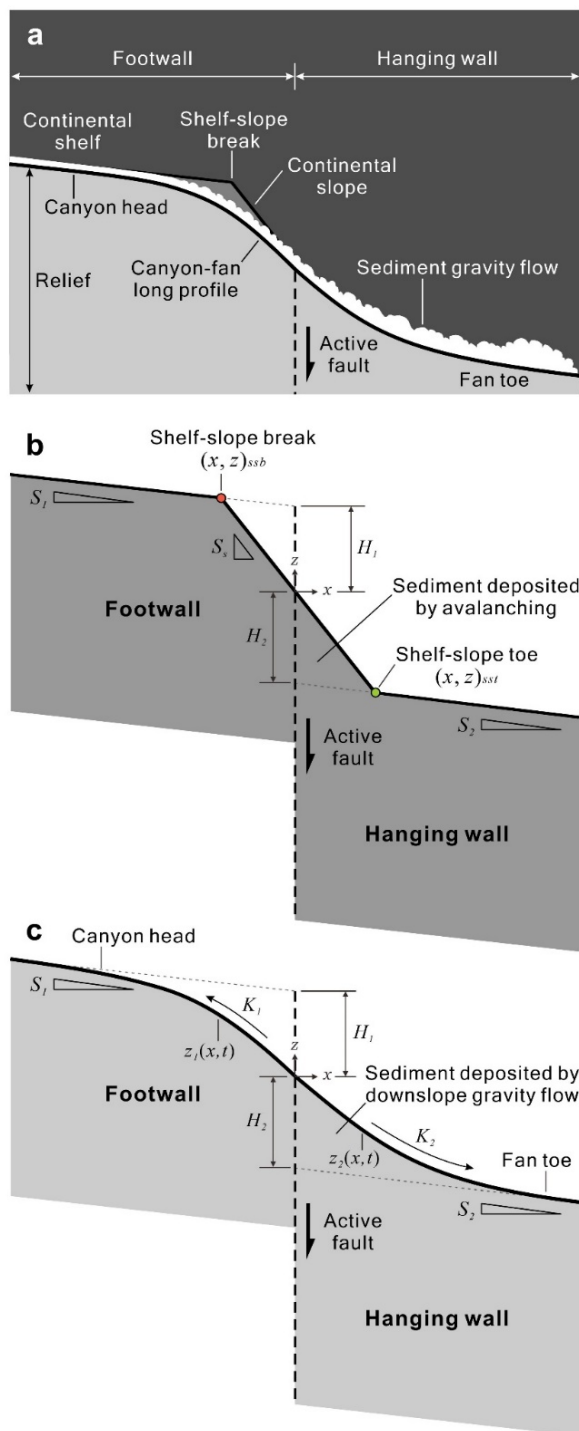


**Figure 3. (a) Geomorphic components for a one-dimensional evolving submarine canyon-fan long system. (b) Mathematical definitions for an evolving continental slope governed by gravity-induced avalanching process. (c) Mathematical definitions for the canyon-fan long profile driven by downslope gravity flows.**



## 155 3 Results

### 3.1 Evolution of submarine canyon-fan systems

Physical experiments simulated the initiation and evolution of submarine canyon-fan systems driven by downslope gravity flows in normal fault settings (Fig. 4). The fault line was at a fixed location ( $x = 400$  mm) and as the hanging wall started to fall, the continental slope expanded simultaneously both upstream and downstream, but keeping its bed slope at the angle of repose ( $38^\circ$ ). At the same time, saline gravity flows formed submarine canyons and fans on the slope. When  $t = 10$  min, tiny gullies and fans appeared at the base of the continental slope. At  $t = 30$  min, small gullies merged into several shelf-incising canyons and a few slope-confined canyons. When  $t = 40$  min, shelf-incising canyons developed their own tributaries. At  $t = 50$  min, four major submarine canyon-fan systems maintained on the continental slope. At  $t = 70$  min, the four major systems continued to grow, but the slope-confined canyons completely disappeared. At  $t = 80$  min, System C appeared obvious fan terraces. When  $t = 90$  min, System A disappeared, and Systems B and C remained kept as mature shelf-incising canyon-fan systems; System D transformed into a slope-confined canyon-fan system. See Fig. S1, Table S1 and Movie S1 to S6 for detailed evolution processes.

The gradient maps calculated from each DEM demonstrated the morphological responses of submarine canyon-fan systems to the given parameters (Fig. 5). Under fixed inflow discharge, double the fault slip rate reduced the number of canyon-fan systems and made the systems become close-spaced (compare Fig. 5a to Fig. 5b and Fig. 5c to Fig. 5d). On the contrary, at fixed fault slip rate, double the inflow discharge resulted in similar size and number of submarine canyon-fan systems (compare Fig. 5a to Fig. 5c and Fig. 5b to Fig. 5d). When the fault slip rate and inflow discharge were extremely contrasted, the minimum fault slip rate formed a large number of slope-confined canyon-fan systems (Run C1, Fig. 5e). Conversely, the maximum fault slip rate resulted in a single shelf-incising canyon-fan system (Run C2, Fig. 5f) in early stages.

The DEM of differences (DoDs) showed the erosion and deposition patterns of canyons and fans for each stage (Fig. 6). When the inflow discharge was fixed, double the fault slip rate made the incision and deposition depths deeper and thicker, respectively (compare Fig. 6a to Fig. 6b and Fig. 6c to Fig. 6d). Conversely, when the fault slip rate was fixed, double the inflow discharge did not make significant differences to incision and deposition depths (compare Fig. 6a to Fig. 6c and Fig. 6b to Fig. 6d). When the fault slip rate and inflow discharge were extremely contrasted, the depths and volumes generated by the maximum fault slip rate (Run C2) were much larger than that of the minimum fault slip rate (Run C1) (Fig. 6e and Fig. 6f). Generally, the responses of DoDs to given parameters were similar to those responses observed in the gradient maps. The influence of fault slip rate and inflow discharge on the volumes of canyons and fans will be discussed in Section 4.

185



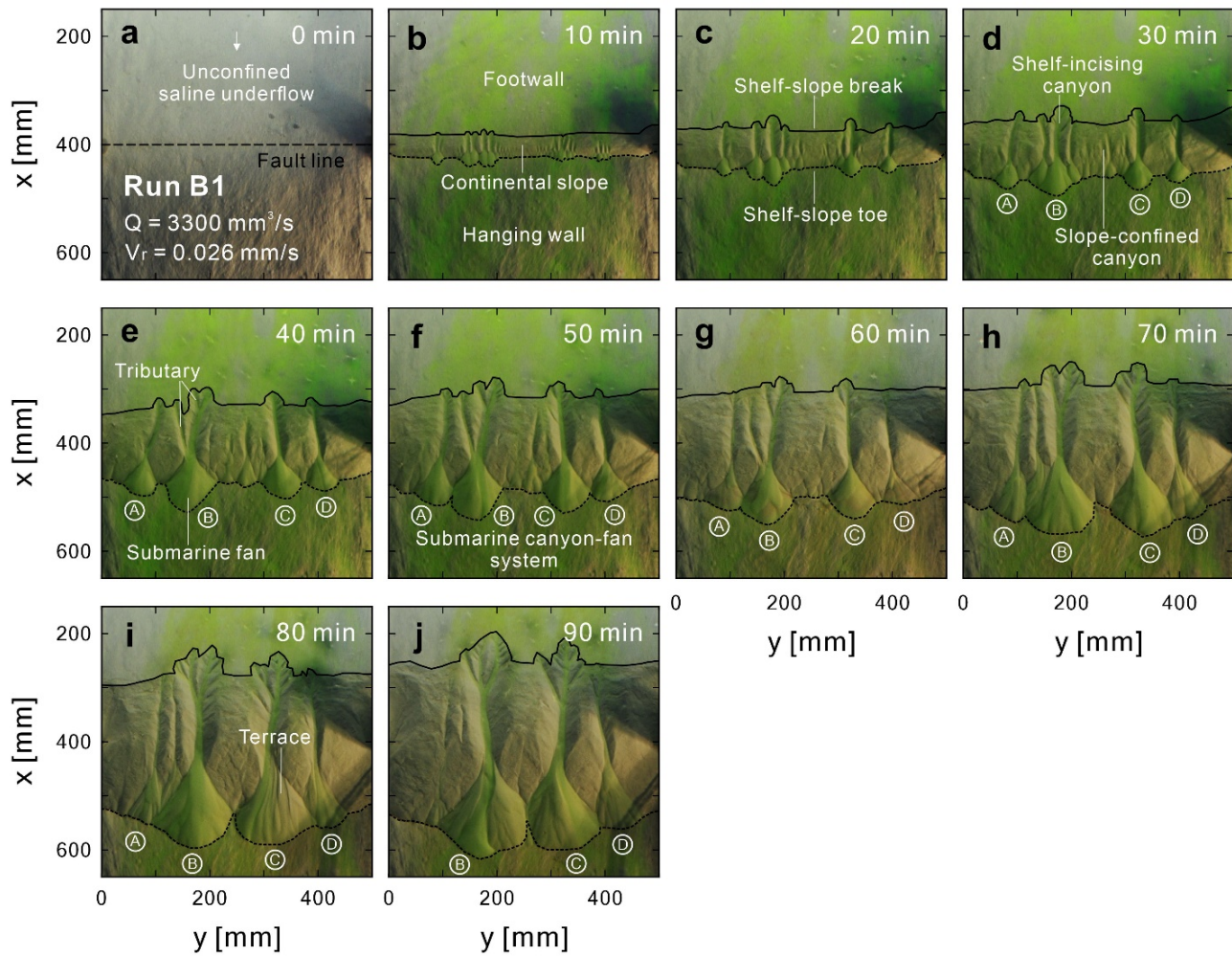


**Figure 4. Observations from the orthophotos (Run B1 from  $t = 0$  to 90 min). Systems A, B, C and D are the traced submarine canyon-fan systems across stages.**

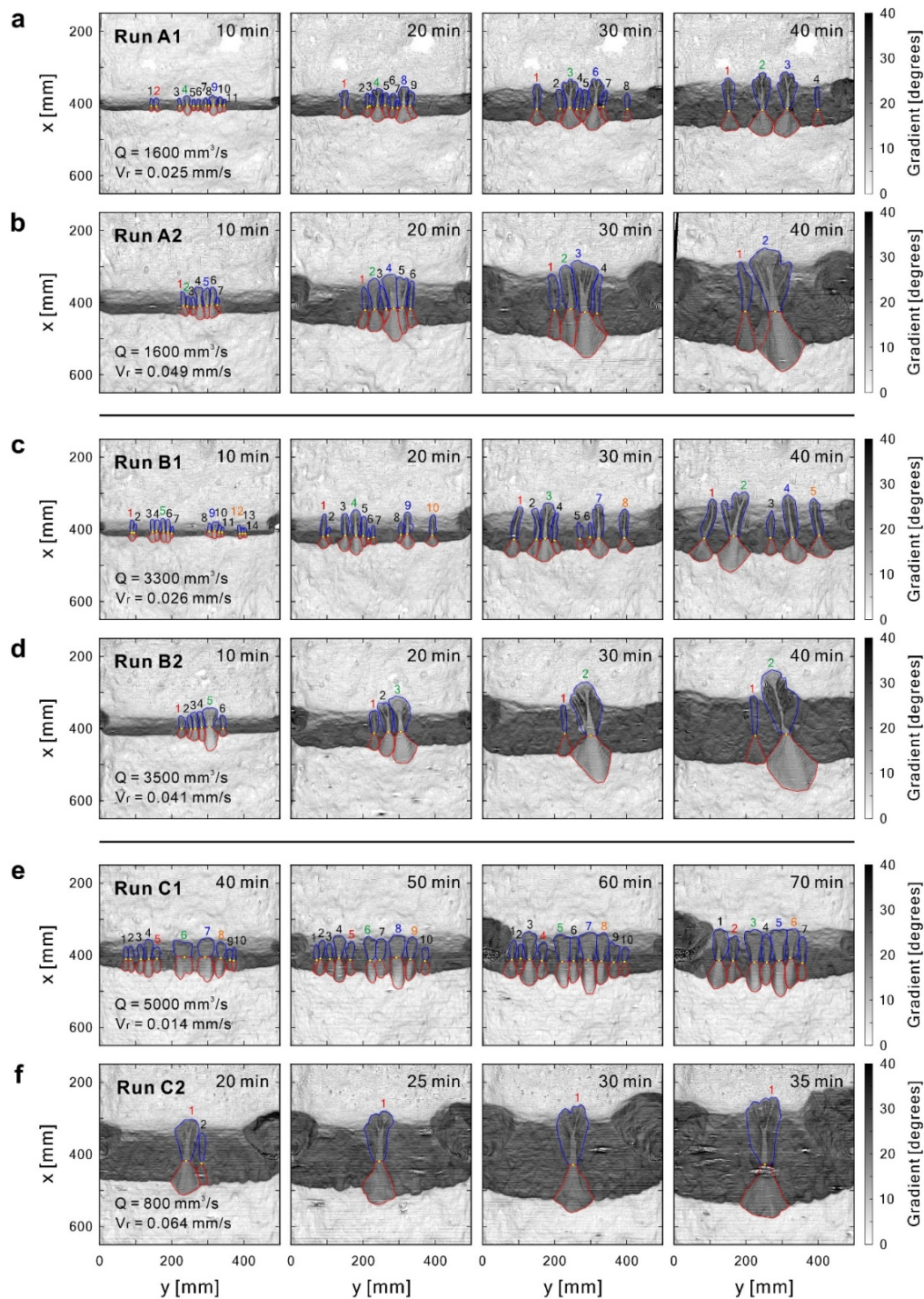


**Figure 5.** Hillshaded gradient maps for each run. Blue lines are the rims of submarine canyons. Red lines are the boundaries of submarine fans. Yellow dots are fan apices. Colored numbers represent the traced canyon-fan system of each stage.



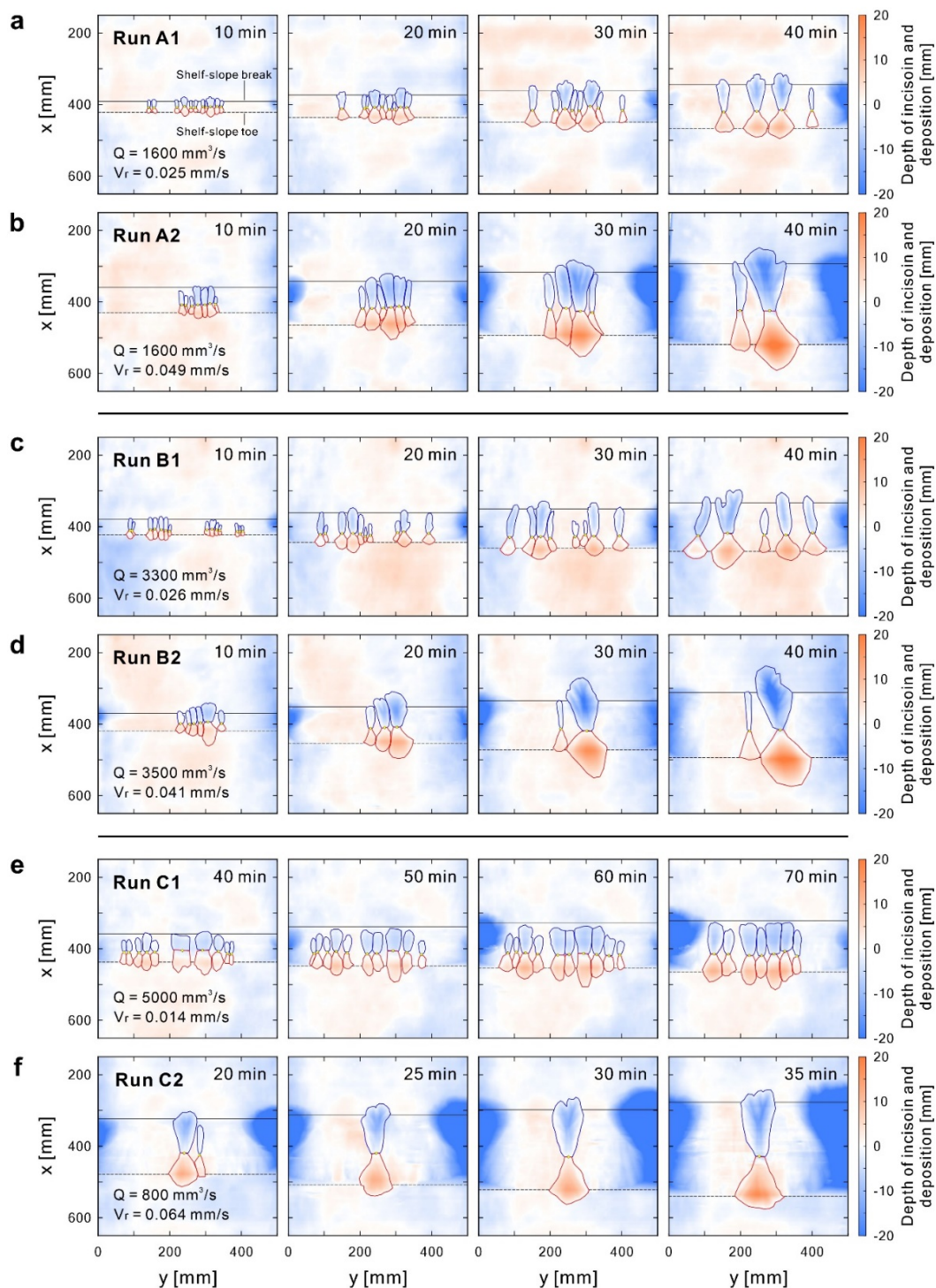


**Figure 6. DEM of differences (DoDs) for each run. The lines of shelf-slope break and shelf-slope toe were translated from the pseudo surface of each run.**



### 3.2 Comparison of submarine canyon-fan long profiles

200 The comparison of experimental and simulated submarine canyon-fan long profiles is shown in Fig. 7. The diffusion model captured the evolution of four major shelf-incising canyon-fan long profiles. The diffusion coefficients  $K_1$  and  $K_2$  controlled the long profile of canyon and fan, respectively. As the hanging wall continued to fall, the canyon-fan long profile became smoother, indicating that the diffusion coefficients were not fixed values, but proportional to the knickpoint heights ( $H_1$  and  $H_2$ ). Contrary to the canyon-fan long profiles, the continental slope was steep, straight and maintained at the angle of repose. The geometric relationship (Eq. (1) and Eq. (2)) well captured the evolution of continental slopes (Fig. 7e). Therefore, both  
205 the diffusion model and geometric relationships capture the essence of submarine canyon-fan systems on an evolving continental slope.

The trajectories of internal moving boundaries over time are shown in Fig. 8. The  $x$ -position of the four moving boundaries were shifted to the fault line ( $x = 400$  mm) for distinguishing whether canyons and fans were in erosion or deposition relative  
210 to the continental slope. The results demonstrated that the trajectories of all internal moving boundaries over time were surprisingly linear. Systems B and C were deep shelf-incising canyons, for which their corresponding canyon incising distance ( $\Delta x_{in}$ ) and fan advancing distance ( $\Delta x_{ad}$ ) were longer. Conversely, Systems A and D were shallow shelf-incising canyons, for which their corresponding  $\Delta x_{in}$  and  $\Delta x_{ad}$  were much shorter. See Fig. S3 for other moving trajectories.

215 On the dimensionless coordinates, both experimental and simulated long profiles showed strong self-similarities (Fig. 9). To investigate the self-similarity of the evolving profiles during different stages of each run, the first and second terms on the right-hand side of Eq. (3) are, respectively, normalized by the shape factor  $H$  and the time-varying length scale  $\sqrt{Kt}$ . That is the upstream and downstream profiles,  $\bar{z}_1(\sigma)$  and  $\bar{z}_2(\sigma)$ , are plotted against the dimensionless coordinates  $\sigma_1$  and  $\sigma_2$ . For instance, the four systems traced in Run B1 at different stages (35 long profiles in total) collapsed to a single curve and showed  
220 strong self-similarity (Fig. 9c). More surprisingly, the scaled submarine canyon-fan long profiles of the other runs also collapsed to a similar theoretical profile, indicating that a morphological self-similarity was established consistently. In addition, the evolving continental slopes of each run also collapsed to the same geometric profile (red solid line). Therefore, these results confirmed that the submarine canyon-fan long profiles and continental slopes evolved at different stages have strong, scale-independent self-similarities.

225

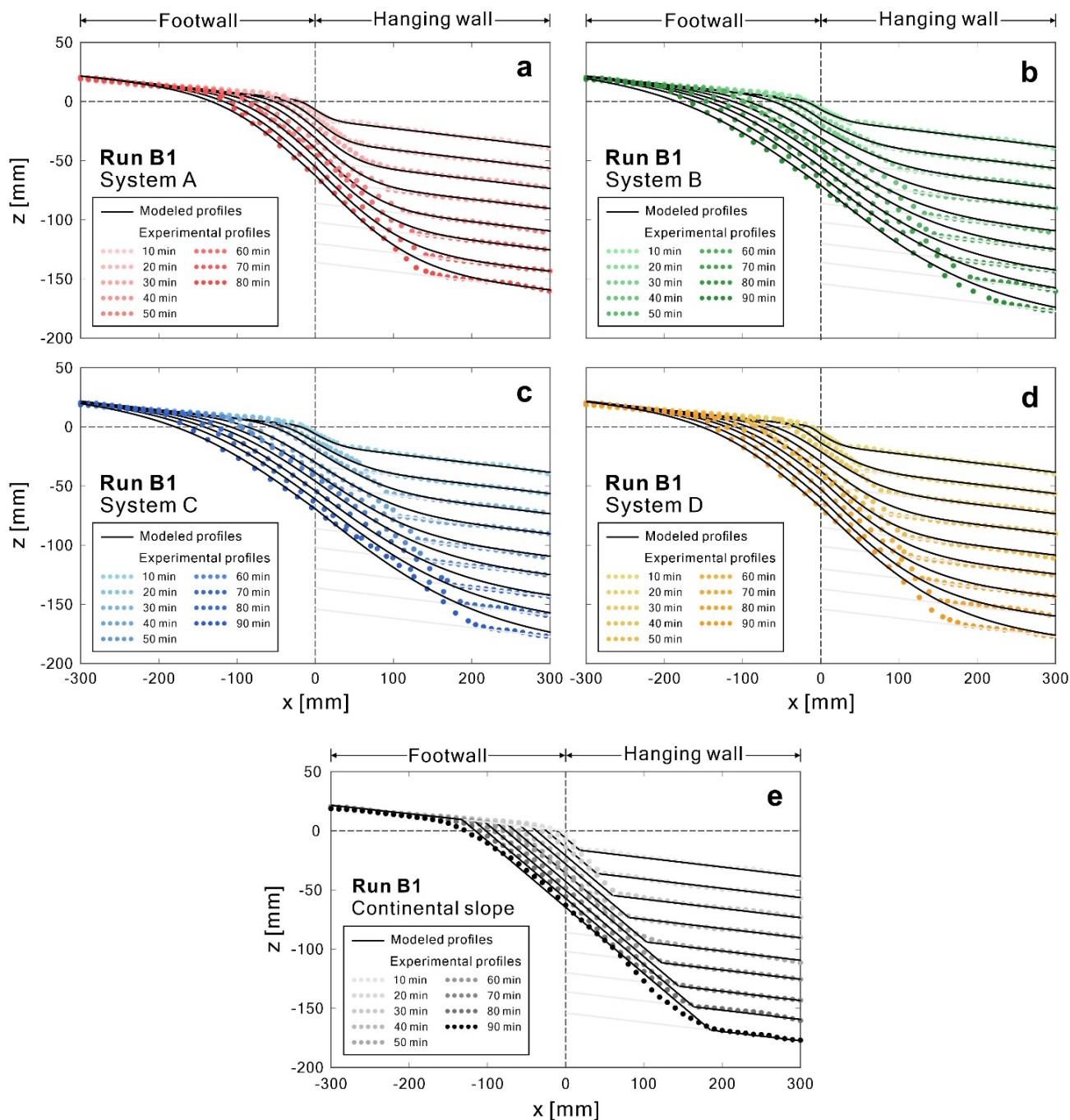
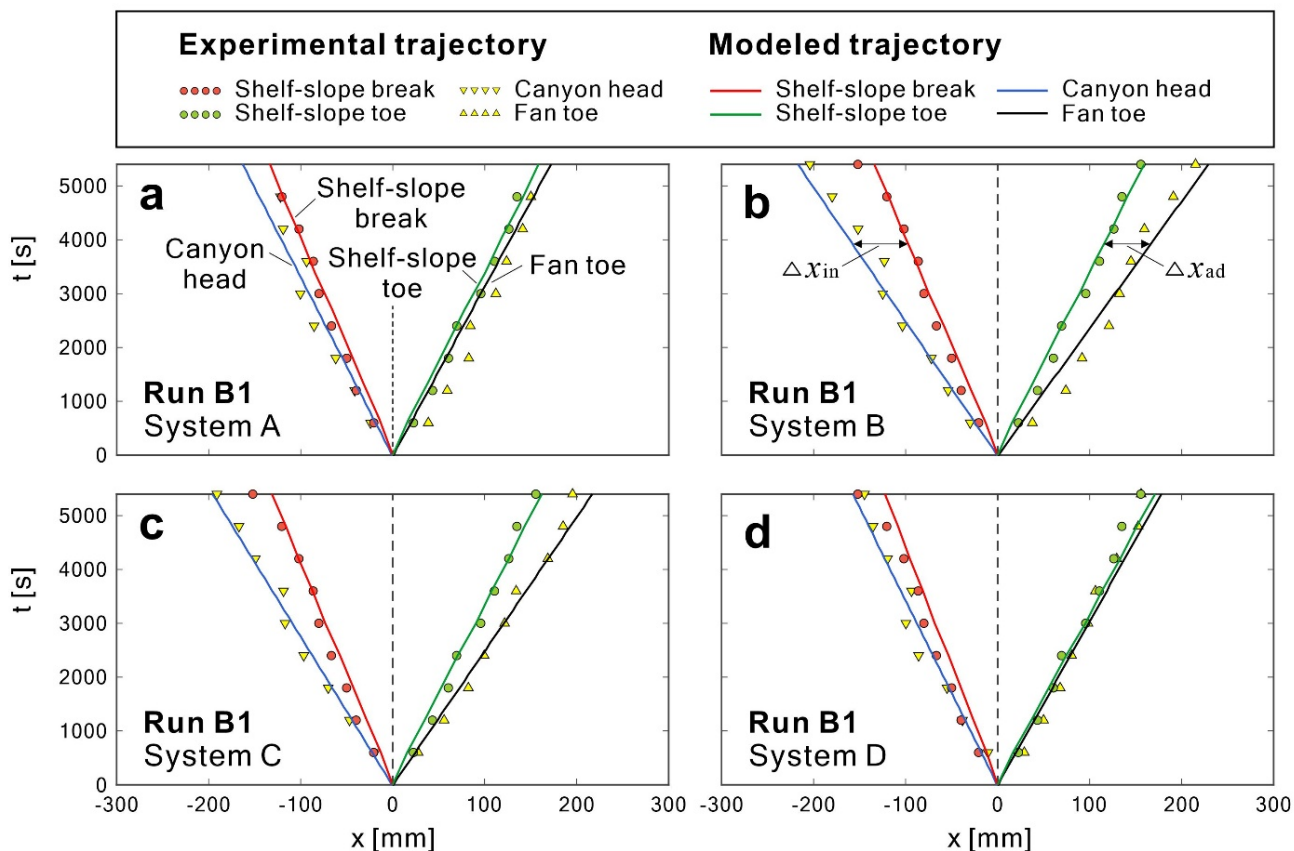
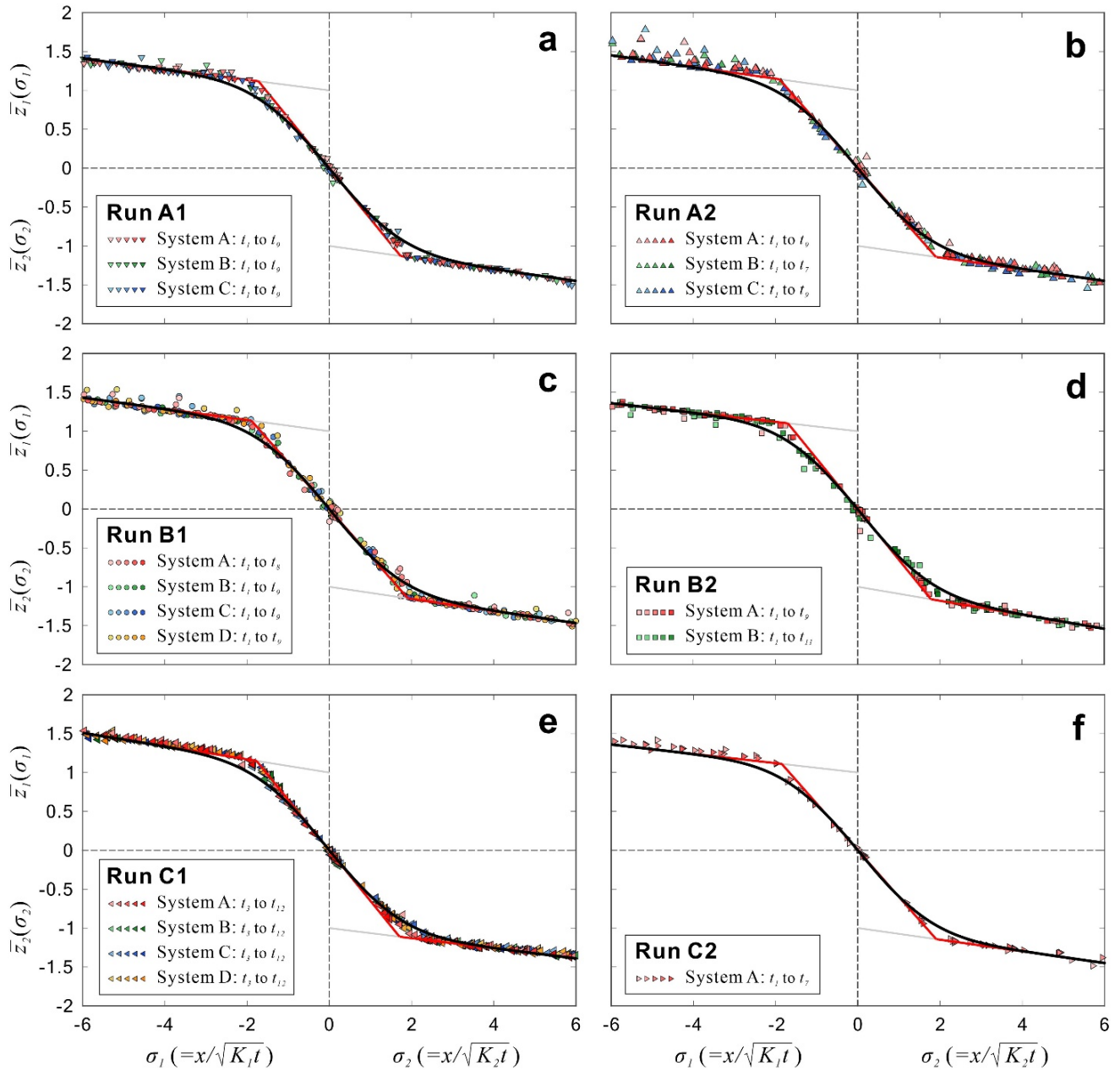


**Figure 7.** Comparisons between experimental and modeled long profiles (for Run B1). (a) to (d) Submarine canyon-fan long profiles of the traced systems at different stages. (e) Continental slope long profiles traced at different stages. See Fig. S2 for long profile comparisons of other runs.



235 **Figure 8.** Comparison between experimental and modeled trajectories of the internal moving boundaries (for Run B1). The shelf-slope break and shelf-slope toe were extracted from the pseudo surface of each stage. Canyon incising distance ( $\Delta x_{in}$ ) is the horizontal distance between the trajectory of canyon head to shelf-slope break. Fan advancing distance ( $\Delta x_{ad}$ ) is the horizontal distance between the trajectory of fan toe to shelf-slope toe.



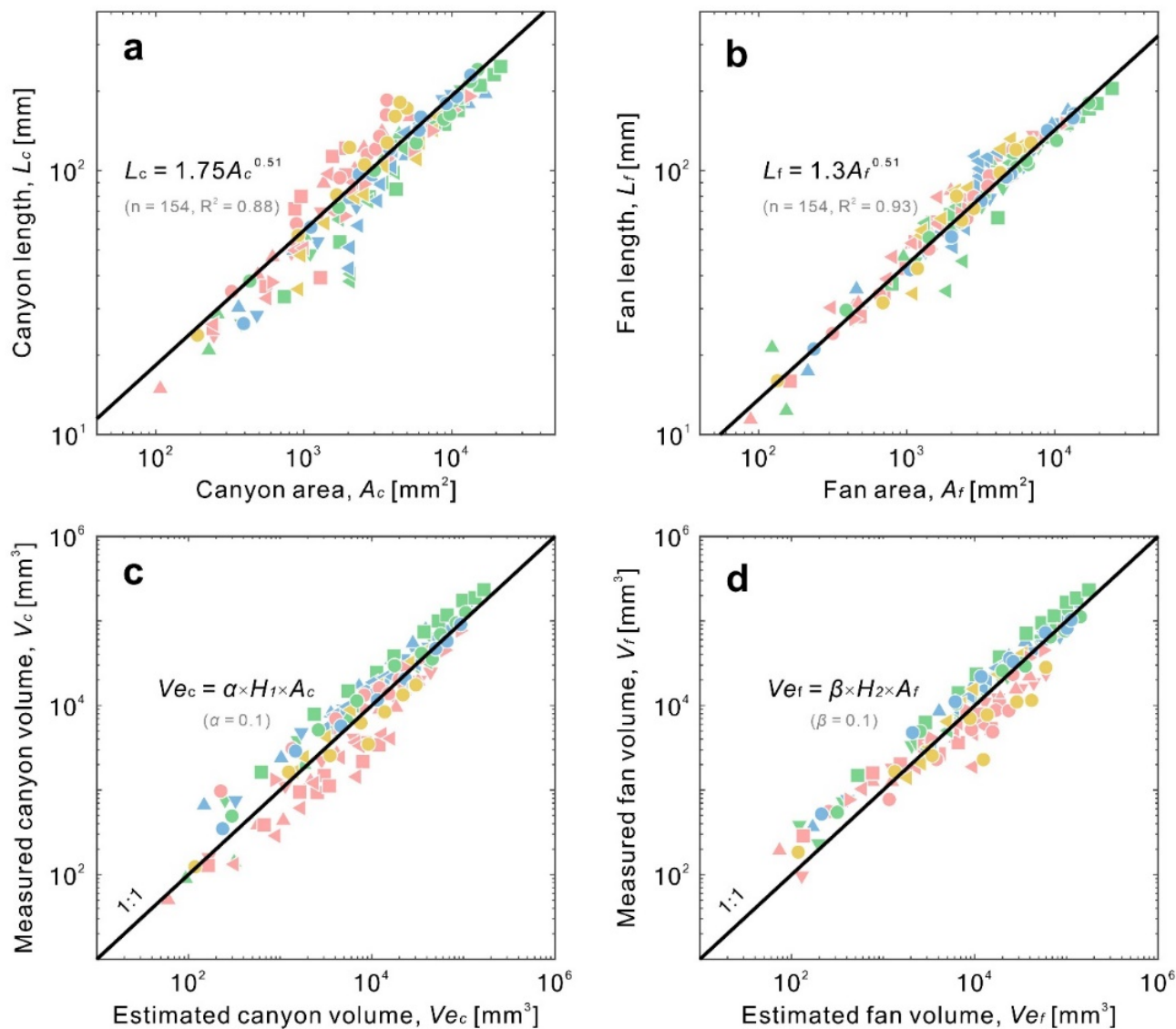


240 **Figure 9. Dimensionless long profiles of each run. Black solid lines are modeled dimensionless canyon-fan long profiles by two-diffusion theory. Red solid lines represent modeled dimensionless continental slopes. Gray solid lines show the normalized step function. Note that the numbers and times of each traced system are not identical.**



### 3.3 Scaling relationships in submarine canyon-fan systems

- 245 Morphometric analyses showed that scaling relationships among submarine canyons and fans were robustly linear (Fig. 10). For instance, the experimental canyon lengths to canyon areas agreed with Hack's scaling relationship (Fig. 10a). Similarly, the scaling relationship was also established in experimental fan lengths to fan areas, with different Hack's coefficients but identical power (Fig. 10b). In addition, the canyon volume ( $V_c$ ) can be estimated from upstream knickpoint height ( $H_1$ ) and canyon area ( $A_c$ ), following the formula  $Ve_c = \alpha \times H_1 \times A_c$ , where  $\alpha$  is a coefficient to be calibrated.
- 250 Equivalently, the fan volume ( $V_f$ ) followed  $Ve_f = \beta \times H_2 \times A_f$ , where  $\beta$  is a coefficient to be calibrated.  $H_2$  is downstream knickpoint height.  $A_f$  is fan area. The results showed that the estimated volumes of canyons had a strong 1 to 1 relationship with the volumes measured directly from the DoDs, giving the coefficient  $\alpha = 0.1$  (Fig. 10c). A similar trend was also established for submarine fans (Fig. 10d), making  $\beta = 0.1$ . These scaling relationships served as the basis for proposing a general rule by using canyon lengths to predict fan volumes, which will be explained in Section 4.



255

**Figure 10. (a-b) The Hack's length to area scaling relationships established for submarine canyons and fans, respectively. (c) 1 to 1 relationship for the estimated to measured volumes of canyons and fans, respectively.**

260

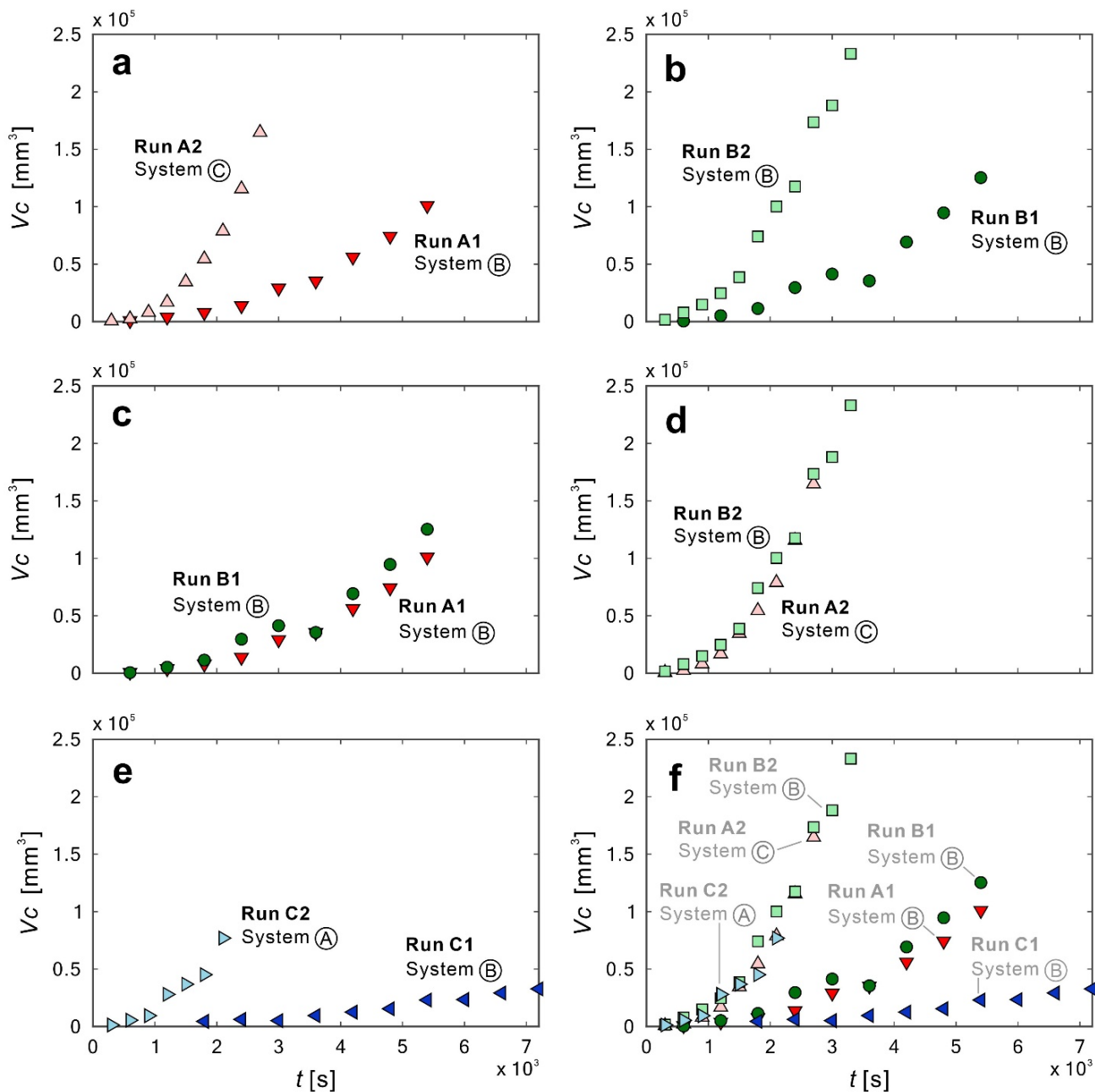


#### 4 Discussion

265 The purpose of this study is to understand the initiation and evolution of fault-controlled submarine canyon-fan systems driven by downslope gravity flows. According to our experimental and modeling results, we propose that the morphological diversity of fault-controlled submarine canyon-fan systems is controlled by fault slip rate and inflow discharge. Scaling relationships revealed in this study support us to establish a general rule for using canyon lengths to predict fan volumes, which greatly increases the applicability of the present work.

270 First, we find that fault slip rates control the merging speed among canyon-fan systems, which in turn affects the number and spacing of the system. A faster fault slip rate generates a greater fault escarpment, which resulted in a stronger retrograding process on the slope. This severer retrograding process facilitates the downslope gravity flows to converge, making the canyon-fan systems to merge rapidly. For instance, under a fixed inflow discharge ( $Q = 1600 \text{ mm}^3/\text{s}$ ), double the fault slip rate (Run A2), the number and spacing were much less than that of Run A1 (Fig. 5a and 5b). Similarly, under an increased inflow discharge ( $Q = 3400 \text{ mm}^3/\text{s}$ ), double the fault slip rate (Run B2), the number and spacing is also much less than that of Run B1 (Fig. 5c and 5d). For the volume of canyon incision, the influence of fault slip rate is significant (Fig. 11a and Fig. 11b). The canyon incision volumes generated by faster fault slip rates is two times larger than that generated by a slower fault slip rate. Our experimental results agree with the idea that canyons in active margins are shorter, steeper, more dendritic and closely spaced (Harris and Whiteway, 2011). We further emphasize that in active margins the fault slip rate controls the merging speed, spacing and quantity of the submarine canyon-fan systems.

285 Second, the length, area and volume of canyons and fans is proportional to inflow discharge, but doubling the inflow discharge has minor influence on its morphology. Larger discharges cause stronger axial incision, triggered more retrograding landslides on canyon-walls, and eventually increased the corresponding lengths, areas and volumes of the systems. For instance, at a fixed fault slip rate ( $0.025 \text{ mm/s}$ ), double the inflow discharge (Run B1), the corresponding size and number are similar to that of Run A1 (Fig. 5a and 5c). Similarly, at an increased fault slip rate ( $0.045 \text{ mm/s}$ ), double the inflow discharge (Run B2), the size and numbers are also similar to that of Run A2 (Fig. 5b and 5d). For the volumes of canyon incision, the influence of inflow discharge was insignificant than that of fault slip rate (Fig. 11c and Fig. 11d). The canyon incision volumes generated by larger inflow discharge are slightly larger than that generated by smaller inflow discharge. Our experimental results agree with that larger discharge forms deeper canyons (Weill et al., 2014). However, we emphasized that the influences due to inflow discharge are insignificant when comparing to the morphological changes caused by fault slip rate.



295 **Figure 11. Effects of fault slip rate and inflow discharge on the volume of evolving submarine canyons. (a-b) Influence of fault slip rate. (c-d) Influence of inflow discharge. (e) Influence of coupled fault slip rate and inflow discharge. (f) Comparison among all runs. All the selected systems were major shelf-incising canyons, except for Run C1, which belonged to slope-confined canyons.**



300 Third, we believe that submarine canyon-fan systems react to coupled fault slip rate and inflow discharge is a competitive  
relationship, rather than a simple positive correlation. Extremely fast slip rate generates fault escarpment rapidly. Thus, if the  
inflow discharge is relatively small, the slope morphologies rapidly merge into a few major shelf-incising canyons. On the  
contrary, slow fault escarpment allow most of the inflow bypass the slope. The corresponding morphologies are slope-confined  
canyons. For instance, the slip rate of Run C2 is 5 times larger than that of Run C1, but the inflow discharge of Run C2 is only  
305 1/6 than that of Run C1. The corresponding canyon lengths and volumes of Run C2 are 5-8 orders larger than those of Run C1  
(Fig. 11e and Fig. 11f). Therefore, we propose that under the coupled effects of fault slip rate and inflow discharge, the final  
slope morphology is dominated by fault slip rate, rather than the inflow discharge.

Specifically, our experimental results may help to interpret the evolution of submarine canyon-fan systems observed on Haida  
310 Gwaii Trough. Although laboratory-scale to field scale are  $10^5$  order different, the morphological characteristics and fault  
settings suggest a similar formation for these two systems. The Haida Gwaii Trough is a bathymetric depression between Haida  
Gwaii Island and Queen Charlotte Terrace, similar to a graben between two normal faults, with different subsidence rates ( $\sim 1$   
mm/yr to 3 mm/yr from north to south, estimated from Harris et al., 2014). Above the fault line, both types of canyons (shelf-  
incising and slope-confined canyons) appear on the continental slope; below the fault line, a series of coalescing submarine  
315 fans are deposited on the Haida Gwaii Trough (Harris et al., 2014b). These morphological characteristics and fault settings are  
similar to our experimental set-up and results. In addition, our experimental videos provide a way to visualize the evolution of  
merging canyons and coalescing fans that are rarely possible to observe in the field. Therefore, we believe that by isolating  
fault slip rate and inflow discharge it is possible to explain the origin and evolution of the submarine canyon-fan systems  
observed on Haida Gwaii Trough.

320  
Finally, we reveal the scaling relationships that link laboratory-scale experiments with field scale submarine canyon-fan  
systems and we propose a general rule to predict fan volumes by simply using canyon lengths. In field-scale submarine canyon-  
fan systems, there are obvious limitations to obtain sediment distributions over time and space. However, our experimental  
canyons and fans show strong Hack's scaling relationships with the Hack's exponent of 0.51. Note that, for instance, the field-  
325 scale Hack's exponent is 1 for the linear canyons and 0.5 for the dendritic canyons on the Atlantic USA continental  
slope (Mitchell, 2005); 0.46 for the canyons in the south Ebro Margin (Micallef et al., 2014); 0.49 for the terrestrial river  
drainage basins (Montgomery and Dietrich, 1992). Combining the Hack's scaling relationship of canyons (Fig. 10a) and the  
strong 1:1 relationship of measured to estimated fan volumes (Fig. 10d), we propose a general rule by using canyon lengths to  
predict fan volumes:

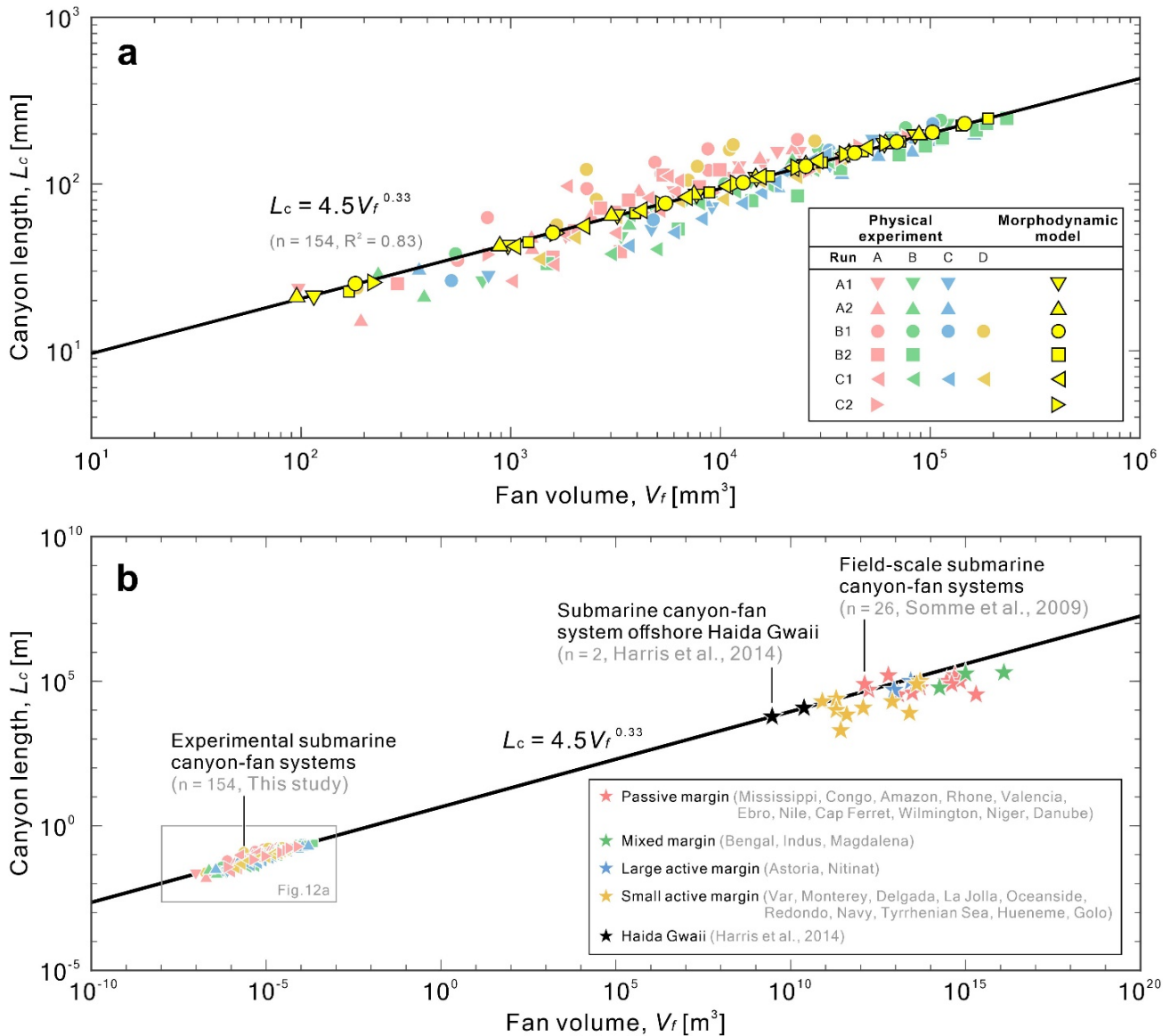
$$330 \quad L_c = 4.5 \cdot V_f^{0.33} \quad (5)$$

where  $L_c$  = canyon length;  $V_f$  = fan volume. This formula is verified by our morphodynamic model (Fig. 12a). We keep this  
verified relationship and compare our experimental data to 26 global source-to-sink systems (Somme et al., 2009) (Fig. 12b).  
We find that this formula is applicable to all observed canyon-fan systems in different margins (passive, mixed and active





margins). The reason is that the evolution of submarine canyons is mainly controlled by increasing reliefs and downslope  
335 gravity flows (Lai et al., 2016). Active margin (through tectonic shortening) or passive margin (by prograding sedimentation  
over a deep basin) are different ways to generate increasing reliefs. The effect is to steepen the continental slope, resulting in  
local oversteepening. When the inflow discharge is fixed, the steepening of the bed slope will increase the dimensionless  
stream power and the sediment transport capability of downslope gravity flows (Lai et al., 2017), i.e., increasing relief is to  
allow the gravity flows to obtain higher potential energy, which is then converted into stronger downslope kinetic  
340 energy. Therefore, we think our experimental approach is universal for all margin types and Eq. (5) is a general rule, which  
spans more than 20 orders from laboratory-scale to margin-scale. By applying Eq. (5) to the canyon-fan systems observed on  
Haida Gwaii Trough (Fig. 1a), considering that the length of the shelf-incising canyon is 12,000 m, the corresponding fan  
volume should be  $24 \times 10^9 \text{ m}^3$ ; if the length of slope-confined canyon is 6,000 m, the fan volume should be  $29.5 \times 10^8 \text{ m}^3$ .  
Therefore, this general rule allows researchers to quickly use canyon lengths to estimate the first-order fan volumes, greatly  
345 improving the value and applicability of this study. It is worth to mention that our approach may not be applicable to the scaling  
relationships between lobes and lobe elements (Pettinga et al., 2018), which focused on the distal part of fan lobes.



350 **Figure 12. (a)** The scaling relationship built from our experimental data and verified by the morphodynamic model. **(b)** The general scaling relationship of canyon lengths to fan volumes among laboratory-scale ( $n = 154$ , this study), margin-scale ( $n = 26$ , [Somme et al., 2009](#)), and offshore Haida Gwaii ( $n = 2$ , [Harris et al., 2014b](#)).



## 355 **5 Conclusions**

Physical experiments and morphodynamic model allow us to better understand the responses of submarine canyon-fan systems to fault slip rates and inflow discharges. The proposed general rule is ready to be applied to field-scale submarine canyon-fan systems. Here are our conclusions:

1. The results of morphometric analyses support that Hack's scaling relationships exist in both laboratory-scale and field  
360 scale submarine canyon-fan systems.
2. The DEM of differences (DoDs) demonstrate the patterns of sediment erosion and deposition and provide reliable volumes of canyons and fans.
3. The validated submarine canyon-fan long profiles show strong self-similarities. The corresponding trajectory of internal moving boundaries over time are surprisingly linear.
- 365 4. We propose that fault slip rate controls the convergence and merging speed of submarine canyon-fan systems, which in turn affects their number and spacing.
5. At a fixed fault slip rate, the lengths, areas and volumes of canyons and fans are proportional to inflow discharge.
6. When considering coupled fault slip rates and inflow discharges, the influence of these two parameters to canyon-fan morphology is a competitive relationship.
- 370 7. Finally, we unveil scaling relationships across laboratory to field scales and propose a general rule to predict fan volumes by using canyon lengths.

We assume that the morphodynamic processes causing the evolution of experimental submarine canyon-fan systems may differ from the field analogues, but we claim and demonstrate that at least we are able to predict the first-order general morphological and sedimentological patterns at basin scale. In short, our findings are inspiring and valuable for field  
375 researchers and/or modelers to better interpret and predict the morphological evolution and sedimentary processes of submarine canyon-fan systems in active fault settings. Next steps will be to consider different fault dip angles and even to explore thrust-fault controlled submarine canyon-fan systems in active convergent margins.

### **Data Availability**

The videos of the experiments are accessible from Zenodo repository at: DOI:10.5281/zenodo.7271139

## 380 **Supplement**

The supplement related to this article is available online at:



### Author contributions

SYJL conceived the idea, performed the experiment and conducted the analysis. SYJL drafted the paper, with contributions from DA, AM, TPG and HC. All authors worked on the submitted final version.

### 385 Competing interests

The authors declare that they have no conflicts of interest.

### Acknowledgements

This study was supported by the Ministry of Science and Technology (MOST), Taiwan (grants to S. Y. J. L.: MOST 109-2628-E-006-006-MY3). We thank Jyun-Fong Jiang for helping with the design of the first version of the experimental  
390 tank. Students of Morphohydraulics Imaging Laboratory (MIL) are also well acknowledged for their help during the experiment runs. D.A. acknowledges the support from the Spanish government through the grants PID2020-114322RBI00 and EIN2020-112179 funded by MCIN/AEI/10.13039/501100011033 and NextGenerationEU, and the Catalan Government Excellence Research Groups Grant to GRC Geociències Marines (ref. 2017 SGR315).

### Financial support

395 This study was supported by the Ministry of Science and Technology (MOST), Taiwan (grants to S. Y. J. L.: MOST 109-2628-E-006-006-MY3).

### References

- Amblas, D. and Dowdeswell, J.: Physiographic influences on dense shelf-water cascading down the Antarctic continental slope, *Earth-Science Reviews*, 185, 887-900, 2018.
- 400 Amblas, D., Gerber, T. P., Canals, M., Pratson, L. F., Urgeles, R., Lastras, G., and Calafat, A. M.: Transient erosion in the Valencia Trough turbidite systems, NW Mediterranean Basin, *Geomorphology*, 130, 173-184, DOI 10.1016/j.geomorph.2011.03.013, 2011.
- Amblas, D., Gerber, T. P., Mol, B., Urgeles, R., Garcia-Castellanos, D., Canals, M., Pratson, L. F., Robb, N., and Canning, J.: Survival of a submarine canyon during long-term outbuilding of a continental margin, *Geology*, 40, 543-546, Doi 10.1130/G33178.1, 2012.
- 405 Barrie, J. V., Conway, K. W., and Harris, P. T.: The Queen Charlotte Fault, British Columbia: seafloor anatomy of a transform fault and its influence on sediment processes, *Geo-Marine Letters*, 33, 311-318, 10.1007/s00367-013-0333-3, 2013.
- Brothers, D. S., Uri, S., Andrews, B. D., Chaytor, J. D., and Twichell, D. C.: Geomorphic process fingerprints in submarine canyons, *Marine Geology*, 337, 53-66, 2013.
- 410 Brothers, D. S., Miller, N. C., Barrie, J. V., Haeussler, P. J., Greene, H. G., Andrews, B. D., Zielke, O., Watt, J., and Dartnell, P.: Plate boundary localization, slip-rates and rupture segmentation of the Queen Charlotte Fault based on submarine tectonic geomorphology, *Earth Planet Sc Lett*, 530, 115882, 2020.
- Canals, M., Puig, P., de Madron, X. D., Heussner, S., Palanques, A., and Fabres, J.: Flushing submarine canyons, *Nature*, 444, 354-357, 10.1038/nature05271, 2006.



- 415 Cantelli, A., Pirmez, C., Johnson, S., and Parker, G.: Morphodynamic and Stratigraphic Evolution of Self-Channelized Subaqueous Fans Emplaced by Turbidity Currents, *Journal of Sedimentary Research*, 81, 233-247, 10.2110/jsr.2011.20, 2011.
- Capart, H., Bellal, M., and Young, D. L.: Self-similar evolution of semi-infinite alluvial channels with moving boundaries, *Journal of Sedimentary Research*, 77, 13-22, 10.2110/jsr.2007.009, 2007.
- 420 Covault, J. A., Fildani, A., Romans, B. W., and McHargue, T.: The natural range of submarine canyon-and-channel longitudinal profiles, *Geosphere*, 7, 313-332, Doi 10.1130/Ges00610.1, 2011.
- Dadson, S., Hovius, N., Pegg, S., Dade, W. B., Horng, M. J., and Chen, H.: Hyperpycnal river flows from an active mountain belt, *J. Geophys. Res.-Earth Surf.*, 110, 2005.
- Fernandez, R. L., Cantelli, A., Pirmez, C., Sequeiros, O., and Parker, G.: Growth Patterns of Subaqueous Depositional Channel Lobe Systems Developed Over A Basement With A Downdip Break In Slope: Laboratory Experiments, *Journal of Sedimentary Research*, 84, 168-182, 10.2110/jsr.2014.10, 2014.
- 425 Foreman, B. Z., Lai, S. Y. J., Komatsu, Y., and Paola, C.: Braiding of submarine channels controlled by aspect ratio similar to rivers, *Nat. Geosci.*, 8, 700+, 10.1038/NNGEO2505, 2015.
- Gerber, T. P., Amblas, D., Wolinsky, M. A., Pratson, L. F., and Canals, M.: A model for the long-profile shape of submarine canyons, *J. Geophys. Res.-Earth Surf.*, 114, Artn F03002, Doi 10.1029/2008jf001190, 2009.
- 430 Hack, J. T.: *Studies of longitudinal stream profiles in Virginia and Maryland*, US Government Printing Office 1957.
- Hanks, T. C., Bucknam, R. C., Lajoie, K. R., and Wallace, R. E.: Modification of wave-cut and faulting-controlled landforms, *Journal of Geophysical Research: Solid Earth*, 89, 5771-5790, 1984.
- Harris, P. T. and Whiteway, T.: Global distribution of large submarine canyons: Geomorphic differences between active and passive continental margins, *Marine Geology*, 285, 69-86, 2011.
- 435 Harris, P., Macmillan-Lawler, M., Rupp, J., and Baker, E. J. M. G.: Geomorphology of the oceans, 352, 4-24, 2014a.
- Harris, P. T., Barrie, J. V., Conway, K. W., and Greene, H. G.: Hanging canyons of Haida Gwaii, British Columbia, Canada: Fault-control on submarine canyon geomorphology along active continental margins, *Deep Sea Research Part II: Topical Studies in Oceanography*, 104, 83-92, 10.1016/j.dsr2.2013.06.017, 2014b.
- 440 Hasbargen, L. E. and Paola, C.: Landscape instability in an experimental drainage basin, *Geology*, 28, 1067-1070, 2000.
- Horton, R. E.: Erosional development of streams and their drainage basins; hydrophysical approach to quantitative morphology, *Geological society of America bulletin*, 56, 275-370, 1945.
- Hsieh, Y. h., Liu, C. s., Suppe, J., Byrne, T. B., and Lallemand, S.: The chimei submarine canyon and fan: A record of Taiwan arc-continent collision on the rapidly deforming overriding plate, *Tectonics*, 39, e2020TC006148, 2020.
- 445 Lai, S. Y. J., Samuel S. C. Hung, Brady Z. Foreman, Ajay B. Limaye, and Jean-Louis Grimaud, a. C. P.: Stream power controls the braiding intensity of submarine channels similarly to rivers, *Geophysical Research Letters*, 10.1002/, 2017.
- Lai, S. Y. J. and Wu, F. C.: Two-Stage Transition From Gilbert to Hyperpycnal Delta in Reservoir, *Geophysical Research Letters*, 48, 10.1029/2021gl093661, 2021.
- 450 Lai, S. Y. J., Gerber, T. P., and Amblas, D.: An experimental approach to submarine canyon evolution, *Geophysical Research Letters*, 43, 2741-2747, 2016.
- Métivier, F., Lajeunesse, E., and Cacas, M.-C.: Submarine canyons in the bathtub, *Journal of sedimentary research*, 75, 6-11, 2005.
- Micallef, A., Mountjoy, J. J., Barnes, P. M., Canals, M., and Lastras, G.: Geomorphic response of submarine canyons to tectonic activity: Insights from the Cook Strait canyon system, New Zealand, *Geosphere*, 10, 905-929, 10.1130/ges01040.1, 2014.
- 455 Milliman, J. D. and Kao, S. J.: Hyperpycnal discharge of fluvial sediment to the ocean: Impact of Super-Typhoon Herb (1996) on Taiwanese rivers, *Journal of Geology*, 113, 503-516, 2005.



- Mitchell, N. C.: Interpreting long-profiles of canyons in the USA Atlantic continental slope, *Marine Geology*, 214, 75-99, DOI 10.1016/j.margeo.2004.09.005, 2005.
- 460 Mitchell, N. C.: Morphologies of knickpoints in submarine canyons, *Geological Society of America Bulletin*, 118, 589-605, 2006.
- Montgomery, D. R. and Dietrich, W. E.: CHANNEL INITIATION AND THE PROBLEM OF LANDSCAPE SCALE, *Science*, 255, 826-830, 10.1126/science.255.5046.826, 1992.
- Mulder, T. and Syvitski, J. P.: Turbidity currents generated at river mouths during exceptional discharges to the world oceans, *The Journal of Geology*, 285-299, 1995.
- 465 Pettinga, L., Jobe, Z., Shumaker, L., and Howes, N.: Morphometric scaling relationships in submarine channel-lobe systems, *Geology*, 46, 819-822, 10.1130/g45142.1, 2018.
- Prims, J., Furlong, K., Rohr, K., and Govers, R.: Lithospheric structure along the Queen Charlotte margin in western Canada: Constraints from flexural modeling, *Geo-Marine Letters*, 17, 94-99, 1997.
- 470 Puig, P., Palanques, A., and Martín, J.: Contemporary sediment-transport processes in submarine canyons, *Annu Rev Mar Sci*, 6, 53-77, 2014.
- Sequeiros, O. E., Spinewine, B., Beaubouef, R. T., Sun, T. A. O., Garcia, M. H., and Parker, G.: Bedload transport and bed resistance associated with density and turbidity currents, *Sedimentology*, 57, 1463-1490, 10.1111/j.1365-3091.2010.01152.x, 2010.
- 475 Spinewine, B., Sequeiros, O. E., Garcia, M. H., Beaubouef, R. T., Sun, T., Savoye, B., and Parker, G.: Experiments on Wedge-Shaped Deep Sea Sedimentary Deposits in Minibasins and/or on Channel Levees Emplaced by Turbidity Currents. Part II. Morphodynamic Evolution of the Wedge and of the Associated Bedforms, *Journal of Sedimentary Research*, 79, 608-628, Doi 10.2110/Jsr.2009.065, 2009.
- Strahler, A. N.: Quantitative analysis of watershed geomorphology, *Eos, Transactions American Geophysical Union*, 38, 913-920, 1957.
- 480 Straub, K. M., Jerolmack, D. J., Mohrig, D., and Rothman, D. H.: Channel network scaling laws in submarine basins, *Geophysical Research Letters*, 34, 10.1029/2007gl030089, 2007.
- Talling, P. J., Allin, J., Armitage, D. A., Arnott, R. W. C., Cartigny, M. J. B., Clare, M. A., Felletti, F., Covault, J. A., Girardclos, S., Hansen, E., Hill, P. R., Hiscott, R. N., Hogg, A. J., Clarke, J. H., Jobe, Z. R., Malgesini, G., Mozzato, A., Naruse, H., Parkinson, S., Peel, F. J., Piper, D. J. W., Pope, E., Postma, G., Rowley, P., Sguazzini, A., Stevenson, C. J., Sumner, E. J., Sylvester, Z., Watts, C., and Xu, J. P.: Key Future Directions for Research on Turbidity Currents and Their Deposits, *Journal of Sedimentary Research*, 85, 153-169, 10.2110/jsr.2015.03, 2015.
- 485 Tubau, X., Lastras, G., Canals, M., Micallef, A., and Amblas, D.: Significance of the fine drainage pattern for submarine canyon evolution: The Foix Canyon System, Northwestern Mediterranean Sea, *Geomorphology*, 184, 20-37, 10.1016/j.geomorph.2012.11.007, 2013.
- 490 Weill, P., Lajeunesse, E., Devauchelle, O., Metiver, F., Limare, A., Chauveau, B., and Mouaze, D.: Experimental Investigation on Self-Channelized Erosive Gravity Currents, *Journal of Sedimentary Research*, 84, 487-498, Doi 10.2110/Jsr.2014.41, 2014.
- 495 Yu, B., Cantelli, A., Marr, J., Pirmez, C., O'Byrne, C., and Parker, G.: Experiments on self-channelized subaqueous fans emplaced by turbidity currents and dilute mudflows, *Journal of Sedimentary Research*, 76, 889-902, 2006.